1 decreased by 14%, while the relative extension limit did not differ from the control, similar to the same parameters of fragment 2. The distribution of the values of maximum load and relative extension limit for both intestinal fragments varied considerably in control and vagotomized animals throughout the experiment (Table 1). It can be hypothesized that the rise of mechanical resistance of the intestine in vagotomized animals is due to the connective tissue growth (fibrosis), while the decrease is related to dystrophy of structural components of the intestine, primarily, its muscular layer. Analogous alterations were described for the duodenum in truncal vagotomy in dogs [1]. Nonphysiological activation of lipid peroxidation in biological membranes probably also modifies structural and functional properties of the small intestine, since lipid peroxidation is known to affect mechanical characteristics of various cells, tissues, and organs.

REFERENCES

1. V. A. Kotel'nikov, in: *Surgical Correction of Diseases of the Peritoneal Cavity* [in Russian], Sverdlovsk (1966), p. 17.
2. I. Littman, *Operative Surgery* [in Russian], Budapest (1989).
3. F. Z. Meerson, *Pathogenesis and Prevention of Stress- and Ischemia-Induced Damage to the Heart* [in Russian], Moscow (1984).
4. V. Z. Parton and E. M. Morozov, *Mechanics of Elastic Break* [in Russian], Moscow (1985).
5. R. B. Strelkov, *Statistical Tables for Express Analysis of Experimental and Clinical Material* [in Russian], Obninsk (1980).
6. P. Latimer and C. Eubanks, *Arch. Biochem. Biophys.*, **98**, 274-285 (1962).

Hydrodynamic Reasons for Choosing a Variant of Cavapulmonary Anastomosis

L. A. Bokeria, L. A. Roeva, K. V. Shatalov, and R. R. Movsesyan

Translated from *Byulleten' Eksperimental'noi Biologii i Meditsiny*, Vol. 123, No. 4, pp. 476-480, April, 1997
Original article submitted June 20, 1996

In order to optimize the technique of cavapulmonary anastomosis and to determine mutual position and orientation of the inflow and outflow axes of implanted anastomoses, hemohydrodynamic studies are carried out using laser Doppler anemometry. The most hydrodynamically optimal variant of the cavapulmonary bypass, a crucial anastomosis with a half-diameter shift and an angle of 60° with the outflow axis, is determined.

Key Words: *optimization; vortex formation; turbulence*

One of the most important problems of cardiosurgery is the study of blood flow in the branched vascular bed.

The total cavapulmonary bypass (TCB) was developed as an alternative for cardiopulmonary bypass in patients with congenital heart failure with critically decreased pulmonary circulation [1,5,6].

The TCB is based on the separation of venous and arterial blood through creation of a bypass around the right heart and forcing passive pulmonary circulation [3-5].

A. N. Bakulev Center of Cardiovascular Surgery, Russian Academy of Medical Sciences, Moscow

The aim of the present study was to choose hemodynamically optimal variant of anastomosis in TCB ensuring an adequate pulmonary circulation.

MATERIALS AND METHODS

The study of flow structure in modeled vascular bed in TCB was carried out using laser knife and laser Doppler anemometry techniques.

Noninvasive methods (laser Doppler anemometry) allowed us to develop a new instrument for measurement of flow rate in the given point.

This method offers the following advantages:

0007-4888/97/0004-0414$18.00

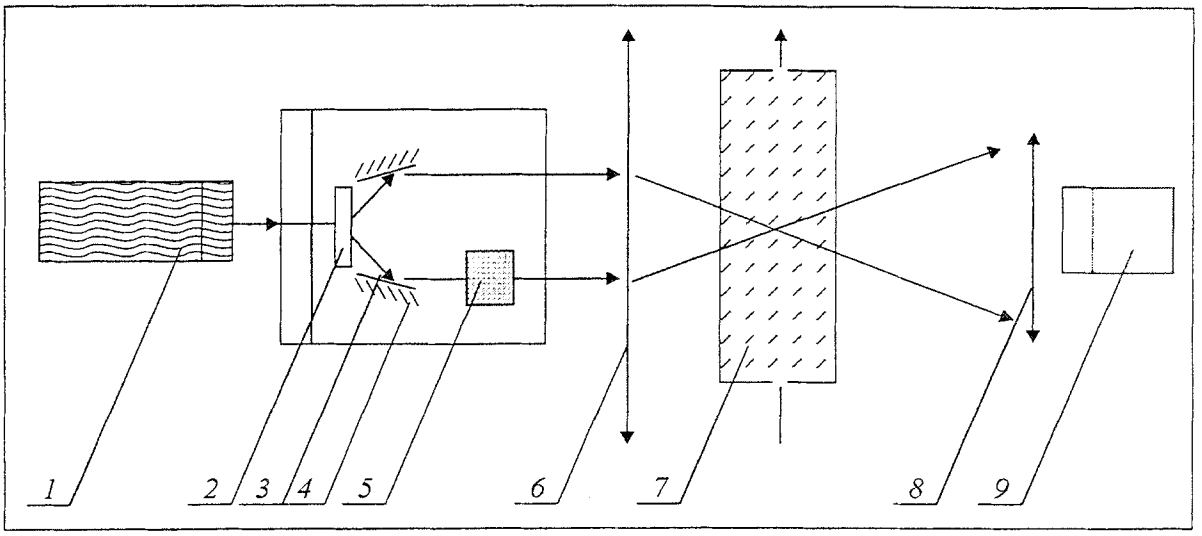

Fig. 1. Differential scheme of laser Doppler anemometry. *1*) laser; *2*) beam-splitting system; *3* and *4*) mirrors; *5*) frequency modulator; *6* and *8*) focusing lenses; *7*) flow field; *9*) detector.

— it causes no turbulence in the flow;
— provides high spatial and temporal resolution;
— requires no calibration;
— flow rate component in any chosen direction can be evaluated;
— the output signal is proportional to the flow rate;
— the possibility of measuring a wide range of flow rates in the presence of retrograde flow.

Laser Doppler anemometer is based on the principle of a frequency shift in the light scattered by particles moving in a flow.

The experimental setup used for the study of the fluid flow in modeled vascular bed in TCB was described in our previous report [2].

Flow rate was determined by measuring the volume passing through the measuring part during a certain period; the Reynolds number (Re) ranged within 100-500, i.e., was close to physiological values in human blood: $Re=Vd/\eta$, where V is the mean flow rate, d is the vessel diameter, and η is kinematic viscosity of the fluid.

The studied rigid model was placed into a cuvette with flat glass walls filled with the working fluid to

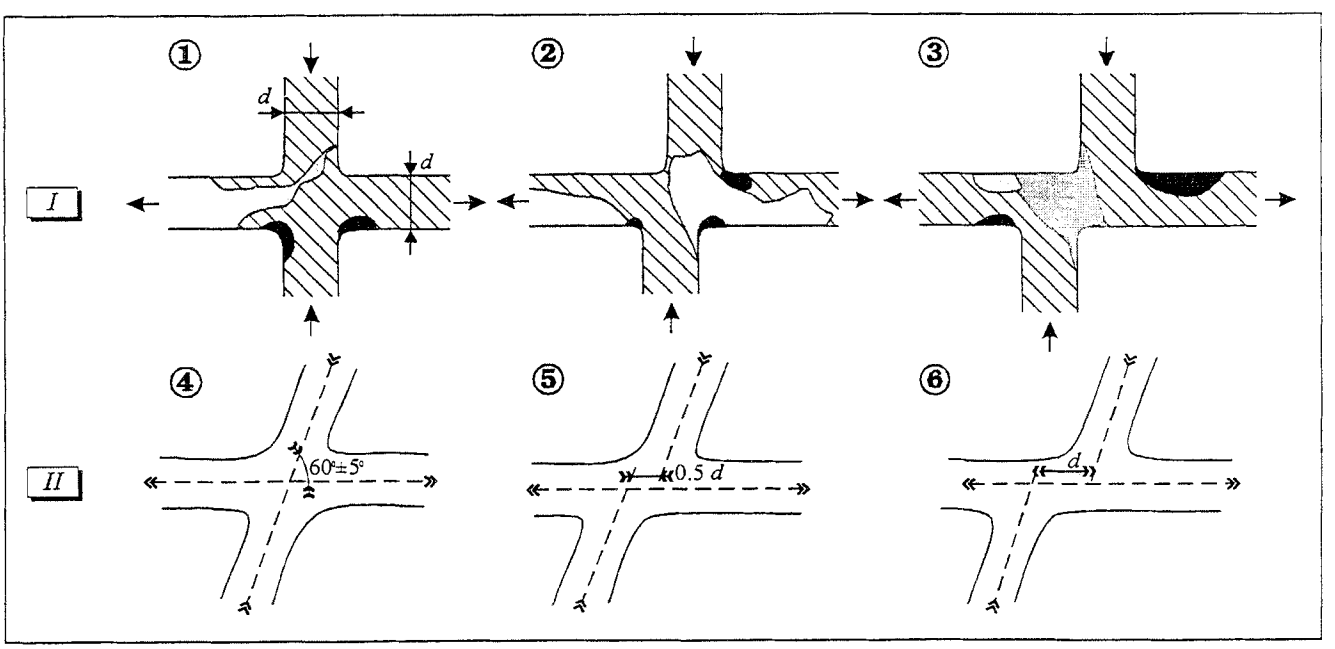

Fig. 2. Models of different relative positions of anastomotic vessels. *I*: coaxial position: *1*) without shift of inflow and outflow axes; *2*) with a 0.5-d shift; *3*) with a 1-d shift; *II*: vessels arranged at an angle to each other: *4*) without shift of inflow and outflow axes; *5*) with a 0.5-d shift; *6*) with a 1-d shift. Dark and gray zones show different degree of turbulence. Flow directions are shown with arrows.

avoid aberrations and refraction at the glass-fluid interface. This allowed us to perform measurements throughout the flow field.

Local flow rates were measured using a DISA laser Doppler anemometer.

Latex particles (no larger than 1 μ) added to the working fluid (distilled water) served as scattering centers; the difference between the flow and particle velocity did not exceed 1%. The measurements were performed in a direct scattering mode using a differential scheme (Fig. 1). Two coherent beams of the same intensity were focused in the studied flow region. The scattered light was collected by the objective and directed to a detector. A laser scalpel method was used for visualization of the flow. A laser beam (LG-69 argon or LTI-701 solid-state laser) passed through a long-focus spherical lens, fell on a cylindrical mirror, and formed an illuminated plane in the studied flow region, the beam width being no more than 0.5 mm. A fluorescent agent was injected into the working fluid as specified below. LG-69 and LTI-701 lasers emitted at major wavelengths of 448 and 532 nm, respectively; the width of the laser scalpel was 3 mm. The fluorescent fluids (laser dyes) used in the study were sodium fluorescein and rhodamine 6G with emission wavelengths of 518 and 570 nm, respectively.

Experiments were carried out at two flow rate values:

1) Q=3.5 liter/min; in these experiments the dye was injected at a distance of 15-25 vessel diameters from the model (Re=2300);
2) Q=1.6 liter/min; in this case the dye was injected directly into the model (Re=1070).

The dye distribution pictures were recorded by a camera, and flow cinegrams were obtained, which allowed us to monitor vortex formation and flow separation in a three- dimensional flow in modeled vascular bed in TCB.

Six vessel models corresponding to different variants of the anastomosis were constructed on the basis of anthropometrical data (Fig. 2).

Thus, we evaluated modern experimental methods of the study of the flow of a viscous fluid which provide quantitative and qualitative determination of the flow structure in the studied vessels and make it possible to relate the obtained local flow parameters with hemodynamic complications arising from flow irregularities.

RESULTS

After analyzing cinegrams presented in Fig. 3, several general conclusions can be made on the flow struc-

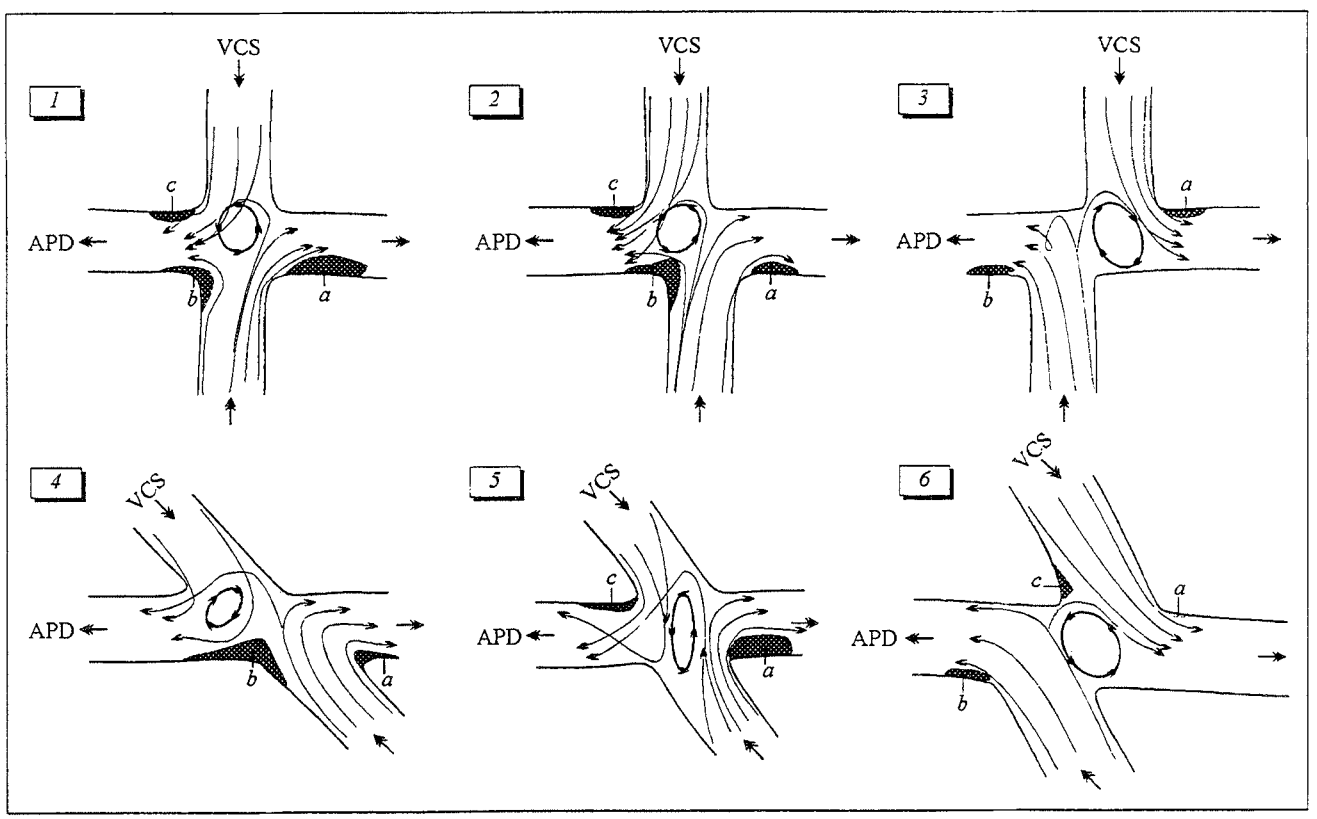

Fig. 3. Visualization of the flow of a viscid fluid in different models. Flow rate Q=3.5 liter/min (*1-3*) and Q=1.6 liter/min (*4-6*). *1*) coaxial arrangement of *a. pulmonalis dextra* (APD) and *v. cava superior* (VCS); *2*) 0.5-d shift of distal and proximal VCS segments; *3*) 1-d shift; *4*) angular coaxial arrangement of VCS and APD; *5*) 0.5-d shift and *6*) 1-d shift of VCS and APD axes; *a-c*: flow separation zones.

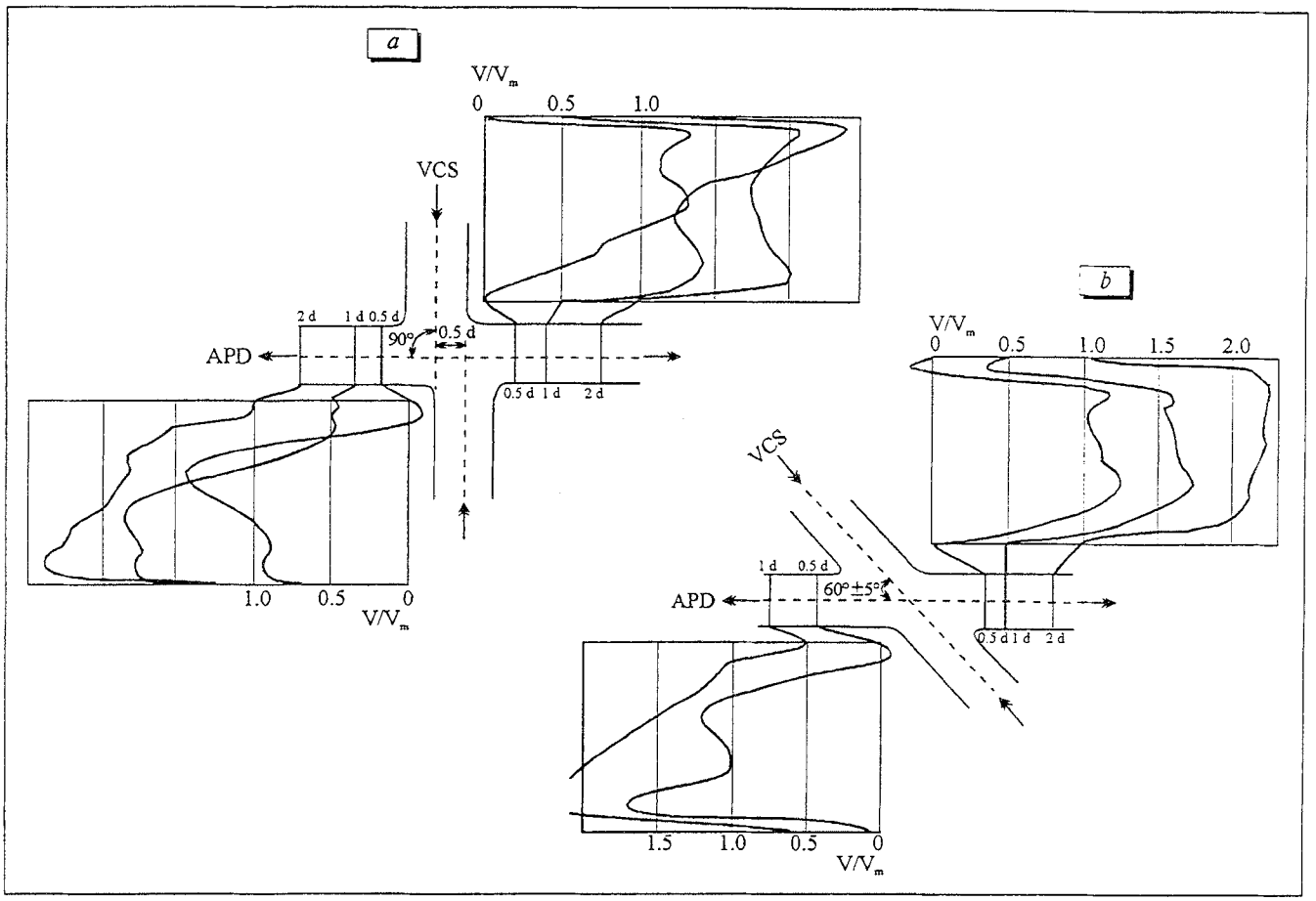

Fig. 4. Flow rate profiles in *a. pulmonalis dextra* (APD) when the APD and *v. cava superior* (VCS) axes are arranged at 90° (*a*) and 60° (*b*).

ture in the studied models. There are three main regions in the flow field: a laminar flow region in the afferent vessels (*v. cava superior*, VCS); a region of stream interaction formed by the afferent vessels; and a region of turbulence in the efferent vessels (*a. pulmonalis dextra*, APD). The regular (laminar) flow in the afferent vessels is confirmed by a stratified pattern of dye distribution in the initial flow observed in all cinegrams.

The region of flow interaction is a three-dimensional turbulent coil. The intensity and the size of the turbulent coil determine fluid redistribution between the efferent vessels (APD). This is an open recirculation zone where the fluid follows helix-like trajectories.

In the efferent vessels, the flow is irregular (turbulent) in nature because of vortex transfer from the vortex coil and due to the fact that the Reynolds numbers are close to critical values. This flow pattern follows from equal dye distribution in flow sections.

In all tested models recirculatory zones adjacent to APD walls were noted (Fig. 3, *a-c*).

The schemes of progressive filling of the flow field with the dye injected pulse-by-pulse into the VCS. The stream interaction zone formed by the initial flows and characterized by additional hydrodynamic resistance are the most prominent on the scheme.

The schemes on Fig. 3 allow one to compare the outflow distribution in the tested models. In model 1 (Fig. 3, *1*), fluid from the distal part of VCS enters both segments of APD, while from the proximal part it enters one segment, which is determined by the interaction zone, in this case an anticlockwise rotating vortex coil. This results in flow deviation to the right and the formation of flow separation areas in the sites of APD—VCS junction.

In model 2 (Fig. 3, *2*), the interaction zone to a greater extent declines the flow from the proximal part of VCS, and only small portion of the fluid ejected by the vortex coil enters the left segment of APD.

In model 3 (Fig. 3, *3*), the interaction zone is less intense than in the previous case and, due to a lower ejecting action, and despite the recirculation zone turning the central vortex clockwise, the fluid from the proximal part of VCS almost completely flows into the left segment of APD.

Figures 3, *1* and *2* show the formation of recirculation zones resulting from flow deviation. Figure 3, *3* demonstrates the formation of a recirculation zone 3 induced by ejecting action of the vortex coil. It should be noted that in model 2 (Fig. 3, *2*) a shift of afferent vessels leads to a lower deviation of both flows and therefore induces smaller recirculation zones *a* and *c* resulting from flow turning. Model 2 is characterized by a greater recirculation zone, since the vortex coil occurring nearby the edge point possess a stronger ejecting effect.

Figure 3, *3* demonstrates the formation of a vortex in the secondary flow. Since the axes of VCS segments are maximally separated from each other, the vortex coil has practically no effect on the fluid flow from VCS, and in this case the recirculation zones caused by turning the flow are minimal.

The flow structure in model 4 is demonstrated in Fig. 3, *4-6*.

The same typical zones in the flow field can be identified. A characteristic feature of this model (the axes of VCS segments are shifted by 0.5±0.1 vessel diameter (d) and arranged at an angle to APD) is a nonstationary migrating vortex coil in the central zone. This can be attributed to the fact that the shift of VCS segments causes opposite sliding flows along the flow boundaries. The vortex coil changes its rotation direction and becomes involved into the transit flow along the APD, while the size of recirculation zones beyond the corners remains little affected.

Figure 4 presents flow velocity profile for the model when the axes of VCS segments are 0.5 d shifted and arranged at an angle to APD. An irregular flow pattern and the presence of reverse velocities confirm the existence and localization of the vortex zones and flow turbulence.

Thus, from hemohydrodynamic point of view, when choosing a variant of anastomosis in the TCB operation, some changes resulting from the nonphysiological blood flow should be taken into account. However, the more comprehensive generalization require additional studies of the degree of flow turbulence in APD and pressure distribution in the vessel walls.

REFERENCES

1. V. P. Podzolkov, M. R. Chiaureli, S. B. Zaets, *et al.*, *Grudn. Serd. Sosud. Khir.*, No. 7, 11-16 (1990).
2. L. A. Roeva, "Construction of prostheses the major elements of the cardiovascular system on the basis of experimental evaluation of hydrodynamics of the heart and great vessel," Author's Synopsis of Doct. Med. Sci. Dissertation [in Russian], Moscow (1990).
3. J. K. Kirklin, E. N. Blackstone, J. W. Kirklin, *et al.*, *J. Thorac. Cardiovasc. Surg.*, **92**, 1049-1064 (1986).
4. M. R. de Leval, P. Kilner, M. Gewilling, and C. Bull, *Ibid.*, **96**, 682-692 (1988).
5. D. D. Mair, V. J. Rice, D. J. Hagler, *et al.*, *Circulation*, **72**, Pt. 2, 88-92 (1985).
6. F. J. Puga, *J. Thorac. Cardiovasc. Surg.*, **98**, 150-154 (1989).